

See discussions, stats, and author profiles for this publication at: <https://www.researchgate.net/publication/50418636>

Improved peptide identification by targeted fragmentation Using CID, HCD and ETD on an LTQ–Orbitrap Velos

ARTICLE *in* JOURNAL OF PROTEOME RESEARCH · MARCH 2011

Impact Factor: 4.25 · DOI: 10.1021/pr1011729 · Source: PubMed

CITATIONS

148

READS

246

8 AUTHORS, INCLUDING:



Marco L Hennrich

European Molecular Biology Laboratory

24 PUBLICATIONS 444 CITATIONS

SEE PROFILE



Dirk Nolting

Thermo Fisher Scientific

21 PUBLICATIONS 852 CITATIONS

SEE PROFILE



Albert J R Heck

Utrecht University

674 PUBLICATIONS 21,767 CITATIONS

SEE PROFILE



Shabaz Mohammed

University of Oxford

157 PUBLICATIONS 7,063 CITATIONS

SEE PROFILE

Improved Peptide Identification by Targeted Fragmentation Using CID, HCD and ETD on an LTQ-Orbitrap Velos

Christian K. Frese,^{†,‡} A. F. Maarten Altelaar,^{†,‡} Marco L. Hennrich,^{†,‡} Dirk Nolting,[§] Martin Zeller,[§] Jens Griep-Raming,[§] Albert J. R. Heck,^{†,‡} and Shabaz Mohammed^{*,†,‡}

[†]Biomolecular Mass Spectrometry and Proteomics Group, Bijvoet Center for Biomolecular Research and Utrecht Institute for Pharmaceutical Sciences, Utrecht University, Padualaan 8, 3584 CH Utrecht, The Netherlands

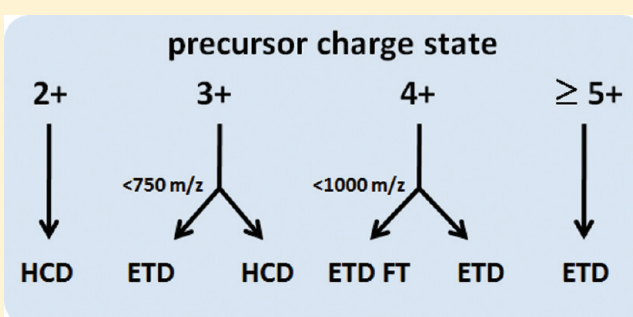
[‡]Netherlands Proteomics Centre, Padualaan 8, 3584 CH Utrecht, The Netherlands

[§]Thermo Fisher Scientific, Bremen, Germany

S Supporting Information

ABSTRACT: Over the past decade peptide sequencing by collision induced dissociation (CID) has become the method of choice in mass spectrometry-based proteomics. The development of alternative fragmentation techniques such as electron transfer dissociation (ETD) has extended the possibilities within tandem mass spectrometry. Recent advances in instrumentation allow peptide fragment ions to be detected with high speed and sensitivity (e.g., in a 2D or 3D ion trap) or at high resolution and high mass accuracy (e.g., an Orbitrap or a ToF). Here, we describe a comprehensive experimental comparison of using ETD, ion-trap CID, and beam type CID (HCD) in combination with either linear ion trap or Orbitrap readout for the large-scale analysis of tryptic peptides. We investigate which combination of fragmentation technique and mass analyzer provides the best performance for the analysis of distinct peptide populations such as N-acetylated, phosphorylated, and tryptic peptides with up to two missed cleavages. We found that HCD provides more peptide identifications than CID and ETD for doubly charged peptides. In terms of Mascot score, ETD FT outperforms the other techniques for peptides with charge states higher than 2. Our data shows that there is a trade-off between spectral quality and speed when using the Orbitrap for fragment ion detection. We conclude that a decision-tree regulated combination of higher-energy collisional dissociation (HCD) and ETD can improve the average Mascot score.

KEYWORDS: ETD, Orbitrap Velos, HCD, data-dependent decision tree, peptide fragmentation



INTRODUCTION

Peptide sequencing is the key step in commonly employed bottom-up approaches within mass spectrometry-based proteomics. Usually proteins are digested with enzymes such as trypsin followed by 1- or 2-dimensional chromatographic separation techniques prior to tandem MS analysis.¹ The current method of choice for peptide sequencing is collision induced dissociation (CID).² Dependent on the instrument type three collision energy regimes can be distinguished. High energy CID (>1 keV) is commonly employed in sector field and TOF/TOF instruments. Low energy CID, which is predominantly applied within proteomics workflows, can be subdivided into resonant-excitation CID (<2 eV; used in ion traps) and beam-type CID (~100 eV; QqQ or QqTOF instruments). In general, the fragmentation process starts with the isolation of the precursor ions followed by collisions with neutral gas atoms, which leads to a conversion of the kinetic energy into internal vibrational energy. As the vibrational energy exceeds a certain threshold, covalent peptide bonds may break. Since the dissociation rate is lower than the energy redistribution rate, the energy is randomly distributed

over all atom bonds. Consequently, it is predominantly the weakest bond that breaks. The resulting fragment ions are used to obtain the peptide sequence by a database search. Resonant excitation, or so-called ion trap CID, differs slightly from beam-type CID. The fragmentation pattern of beam-type CID is due to the higher energy applied and the shorter activation time when compared to ion trap CID. Both b- and y-ions are observed in ion trap CID, whereas the higher energy levels in beam-type CID lead to a predominance of y-ions; b-ions can fragment further to a-ions or smaller species.^{3,4}

Available fragmentation techniques besides CID include electron-based approaches such as electron capture dissociation (ECD) and electron transfer dissociation (ETD).^{5,6} Tandem mass spectrometers enabled with ETD are becoming more popular within the mass spectrometry community due to the technique being implemented on a number of configurations including Q-TOFs,⁷ Q-TRAPs,⁸ linear ion trap-Orbitrap hybrid

Received: November 23, 2010

Published: March 18, 2011

instruments,⁹ and Fourier transform ion cyclotron resonance mass spectrometers.¹⁰ Unfortunately, ECD is currently limited to a few instrument types such as FT-ICR cells or linear ion trap-QTOF instruments since they allow trapping of electrons and analyte cations simultaneously.^{11,12} In contrast to collision induced dissociation, ETD and ECD induce cleavage of the N–C α bond and generate c- and z-type fragment ions. Several studies demonstrated that ETD is particularly useful for peptides with charge states >2.^{13–16} Furthermore, electron driven fragmentation techniques offer advantages for the analysis of acid labile post-translational modifications such as phosphorylation.^{17–19} Overall, it is widely accepted that the outcome of fragmentation upon ETD activation is highly dependent on precursor charge state and that ETD can be used complementary to CID to increase the number of identifications as well as peptide sequence coverage.^{15,16,20,21} In 2008, Coon and co-workers introduced a data-dependent decision tree logic that chooses “on-the-fly” the appropriate activation technique depending on the precursor charge state and *m/z*. The method increases the number of successful MS/MS events and improves the level of protein IDs that one can achieve using a single method.²²

In recent years hybrid tandem mass spectrometers have become available that combine a linear ion trap with an Orbitrap.²³ This combination allows for a high resolution MS spectrum with an excellent mass accuracy in the Orbitrap and the ability to perform rapid MS/MS (several Hz) in the ion trap. Olsen et al. reported in 2007 on the development of the addition of a multipole collision cell to the LTQ-Orbitrap instrument, which then allowed low energy beam-type CID generating spectra similar to those of triple quadrupole and Q-TOF instruments.²⁴ In order to distinguish between ion trap CID and beam type CID performed in the multipole (and to not confuse it with high energy CID), the latter was referred to as higher-energy C-trap dissociation (HCD). Through such an activation process, low mass ions are now observable since there is no 1/3 mass cutoff present for the multipole, which makes it more suitable for the analysis of reporter ions derived from chemical labeling reagents such as iTRAQ or TMT.^{25–28} In 2009, the dual-pressure linear ion trap-Orbitrap became available, which allowed the generation of faster and more efficient ion trap MS/MS. The improvements were made possible through the use of two ion traps operating at different pressure regimes. The instrument was also equipped with a more optimized geometry for HCD transmission and extraction.^{29,30} This instrument has three possible ways of sequencing a peptide: CID, HCD, and ETD. Each has been shown to be very capable, with each having advantages and disadvantages.

The hybrid linear ion trap-Orbitrap instrument is currently one of the most used instruments in high-throughput proteomics and offers multiple peptide fragmentation techniques. Several studies have been performed comparing CID and ETD or CID and HCD. It is widely accepted that CID and ETD can be used complementarily to cover different parts of a complex peptide mixture and to increase sequence coverage.^{15–17,19,20,22,31,32} However, there is still ambiguity whether CID or HCD performs best for peptide identification.^{25,29,33,34} To the best of our knowledge, there is no direct comparison between all three fragmentation techniques in combination with either linear ion trap or Orbitrap detection. Choosing the best fragmentation technique for different populations of peptides is crucial to increase the number of peptides and proteins that can be identified from a complex sample. The recently updated Orbitrap

instrument allows the use of all three fragmentation modes, CID, HCD, and ETD, in combination with either ion trap or Orbitrap mass analysis. Here, we report a comprehensive comparison of all combinations of fragmentation techniques and mass analyzers for peptides derived from a tryptic digest. We analyzed distinct populations of peptides as well as whole cell lysates, and we answer the question of which combination of fragmentation technique and mass analyzer gives the highest number of peptide IDs.

MATERIAL AND METHODS

Sample Preparation

HEK293 cells were cultured at 37 °C and 5% CO₂ in DMEM high glucose medium containing 10% FCS, 10 mM L-glutamine and 5% penicillin/streptomycin (all Lonza). Cells were harvested by trypsinization and washed three times with PBS buffer. Cells were lysed in lysis buffer (8 M urea, 1 tablet Complete Mini EDTA-free Cocktail (Roche), 1 tablet PhosSTOP Phosphatase Inhibitor Cocktail (Roche), in 10 mL 50 mM ammonium bicarbonate buffer) by sonication. The lysate was centrifuged for 15 min at 20,000g, and the supernatant was transferred into new tubes. The BCA assay (Pierce) was used to determine the protein concentration; 2,750 μ g protein was reduced (2 mM dithiothreitol, 25 min at 56 °C) and alkylated (4 mM iodoacetamide, 30 min at room temperature in the dark). Lys-C was added in a 1:75 (w/w) ratio and incubated for 4 h at 37 °C. The sample was diluted four times with 50 mM ammonium bicarbonate buffer. Sequencing grade trypsin (Promega) was added in a 1:100 (w/w) ratio and the incubation was carried out overnight at 37 °C. The digested lysate was desalted by C18 solid phase extraction (Sep-Pak Vac C18 cartridge 3 cc/200 mg, Waters), dried down, and reconstituted in 10% formic acid.

Peptide Fractionation and Mass Spectrometry

Fractionation by low-pH strong cation exchange chromatography was performed as described previously using a Poly-sulfoethyl A column (200 mm \times 2.1 mm, 5 μ m, 200 Å, PolyLC Inc.).³⁵ Collected fractions were dried down in a vacuum concentrator and reconstituted in 100 μ L 10% formic acid. The samples were analyzed on an ETD enabled Orbitrap Velos instrument (Thermo Fisher Scientific, Bremen) connected to an Agilent 1200 HPLC system. All columns were packed in-house. The trap column was made using Aqua C18 material (Phenomenex, Torrance, CA). Reprosil-pur C18 3 μ m (Dr. Maisch, Ammerbuch-Entringen, Germany) was used for the 35 cm analytical column with 50 μ m inner diameter. Solvent A consisted of 0.1 M acetic acid (Merck) in deionized water (Milli-Q, Millipore), and solvent B consisted of 0.1 M acetic acid in 80% acetonitrile (Biosolve). The flow rate of 5 μ L/min was passively split and reduced to an effective flow rate of 100 nL/min. The gradients were as follows: 60 min LC method, 10 min solvent A; 10–40% solvent B within 30 min; 100% solvent B for 2 min; 15 min solvent A. 180 min LC method: 10 min solvent A; 10–25% solvent B within 107 min; 25–50% solvent B within 35 min; 100% solvent B for 2 min; 15 min solvent A. 300 min LC method: 10 min solvent A; 10–23% solvent B within 230 min; 23–50% solvent B within 37 min; 100% solvent B for 2 min; 15 min solvent A. All instrument methods for the Orbitrap Velos were set up in the data dependent acquisition mode. After the survey scan the 10 most intense precursors were selected for subsequent fragmentation using optimal settings for each

Table 1. Orbitrap Velos Parameter Settings of Methods Used for Analyses

mode	Res.	MS2	MS2 activation	Res.	MS2 target		anion target	
	MS	analyzer	(msec)	MS2	AGC	max. inj. (msec)	AGC	max. inj. (msec)
CID	60k	LTQ	10	normal	5000	100	-	-
HCD	30k	FT	0.1	7500	30000	500	-	-
ETD	60k	LTQ	50	normal	5000	100	200000	100
CID FT	30k	FT	10	7500	30000	500	-	-
ETD FT	30k	FT	50	7500	200000	500	400000	200
FT based ddDT	30k	FT (HCD)	0.1	7500	100000	500	-	-
		FT (ETD FT)	50				300000	150
modified ddDT	30k	FT (HCD)	0.1	7500	30000	500	-	-
		LTQ (ETD)	50	normal	5000	100	200000	100
		FT (ETD FT)	50	7500	200000	500	400000	200

activation technique (see Table 1 for parameter details). The normalized collision energy was set to 35% for both CID and HCD. Supplemental activation was enabled for ETD. The signal threshold for triggering an MS/MS event was set to 500 counts. For internal mass calibration the 445.120025 ion was used as lock mass with a target lock mass abundance of 0%. The low mass cutoff for HCD and ETD FT was set to 180 m/z . Charge state screening was enabled, and precursors with unknown charge state or a charge state of 1 were excluded. Dynamic exclusion was enabled (exclusion size list 500, exclusion duration 25 s for the 60 min methods and 90 s for the 180 and 300 min methods). For the decision tree methods the procedures option was enabled. The settings for the FT based decision tree were as follows: ETD was performed instead of HCD if the charge state was 3 and m/z was less than 800, or if the charge state was 4 and the m/z was less than 900, or if the charge state was 5 and m/z was less than 950. The modified decision tree was set up to use ETD with LTQ readout instead of HCD if the charge state was 3 and m/z was less than 750. ETD was performed for all precursor ions with charge states >3 . The fragment ions were analyzed in the Orbitrap instead of the LTQ if the charge state was 4 and m/z was less than 1000. A schematic overview of the modified decision tree algorithm can be found in Supplemental Figure S1. The preview mode option for the survey scan was disabled for both decision tree methods.

Data Analysis

Peak lists were generated from the raw data files using Proteome Discoverer version 1.2 (Thermo Fisher Scientific, Bremen). For the SCX data, one peak list was generated per fragmentation mode. The non-fragment filter was used to simplify ETD spectra with the following settings: the precursor peak was removed within a 4 Da window, charged reduced precursors were removed within a 2 Da window, and neutral losses from charged reduced precursors were removed within a 2 Da window (the maximum neutral loss mass was set to 120 Da). An in-house developed perl script was used to filter CID peak lists (minimum fragment ion count was set to 100, maximum number of fragment ions was set to 100). Peak list files from Orbitrap detection (HCD, CID FT, and ETD FT) were deisotoped and charge deconvoluted, as described elsewhere.³⁶ Briefly, spectra are simplified by removing all except the mono-isotopic peak from isotopic clusters and converting the m/z value of mono-isotopic peaks from higher charged species into the 1+

charged state.³⁷ Peak lists were searched against swissprot (version 56.2, taxonomy filter was set to *Homo sapiens*) including a list of common contaminants using Mascot software version 2.3.02 (Matrix Science, UK). Trypsin was chosen as cleavage specificity with a maximum number of allowed missed cleavages of two. Carbamidomethylation (C) was set as a fixed modification and oxidation (M), acetylation (protein N-term) and phosphorylation (STY) were used as variable modifications. The searches were performed using a peptide tolerance of 50 ppm and a product ion tolerance of 0.6 Da (ion trap readout) and 0.05 Da (Orbitrap readout), respectively. For further filtering the decoy search option was enabled. The resulting dat files were exported and filtered for $<1\%$ false discovery rate at peptide level using in-house developed software "Rockerbox" (version 1.2.6) utilizing the percolator algorithm.³⁸ In brief, percolator extracts features from the dat files and uses a support vector machine to create parsed PSMs.³⁹ Widening the Mascot search space by setting the peptide tolerance to 50 ppm provides a sufficient training data set for the percolator algorithm to distinguish between true positive and decoy hits (Supplemental Figure S2). Hence there is no fixed Mascot score cutoff because peptide matches are accepted until a FDR rate of 1% is reached. However, only PSMs with Mascot scores >20 were accepted to ensure that only high quality data is allowed for this study.

RESULTS AND DISCUSSION

This study was aimed at providing a fair, comprehensive evaluation of all possible combinations of peptide fragmentation techniques and mass spectrometric detection modes and to elucidate the feasibility and performance of each method for efficient, routine peptide sequencing. For the purpose of the evaluation we generated populations of the main peptide compositions generally sequenced by mass spectrometry: N-acetylated peptides, singly phosphorylated, and tryptic peptides with 0, 1, and 2 missed cleavages (5 discrete peptide pools). All peptide pools were generated from a trypsinized HEK293 cell lysate that had been subjected to fractionation by low-pH SCX.^{21,35} These peptide pools were analyzed using a 150 min gradient (180 min total analysis time), and the 10 most intense precursors from each full scan were selected for MS/MS. Each pool was analyzed five times using exclusively either CID or ETD with LTQ mass analysis (referred to as CID, ETD), CID or ETD with Orbitrap readout (CID FT, ETD FT), or HCD (only

Table 2. Number of PSMs and Average Mascot Scores from Analyses of Distinct Peptide Pools Generated by Low-pH SCX Fractionation of a Tryptic HeLa Digest^a

peptide population	CID		ETD		HCD		CID FT		ETD FT	
	PSM	av. score	PSM	av. score	PSM	av. score	PSM	av. score	PSM	av. score
2+	7775	47	5445	43	10869	56	8781	61	4461	44
3+	3309	38	5163	55	6698	58	5488	56	4055	68
4+	573	33	1815	45	2470	52	2068	49	1924	89
N- acetylated	1018	60	583	51	1105	70	1066	75	500	54
phosphorylated	1558	40	1222	44	1982	46	1822	50	1051	47
# spectra	119986		83264		101360		90629		58943	
total PSM	14233		14228		23124		19225		11991	

^a All samples were analyzed consecutively five times by CID, CID FT, HCD, ETD, and ETD FT.

Orbitrap readout available); see Table 1. Example MS base peak chromatograms are available in the Supporting Information (Supplemental Figure S3). The instrument operates in parallel acquisition mode when the LTQ is used for the product ion analysis. This is, of course, not possible for the modes where all scans are carried out in the Orbitrap. The summation of data for each activation method led to an average of ~90,000 spectra (Table 2). We found that the CID LTQ analyses generated the most tandem MS spectra followed by HCD, ETD, CID FT and ETD FT (Table 2). The differences can be directly linked to the use of parallel acquisition and the average scan time duration, which comprises the time for ion accumulation, isolation of the precursor, fragmentation, and detection of the fragment ions. When analyzing the data at the peptide identification level, the data from the HCD analyses provided, by far, the highest number of peptide to spectrum matches (PSMs) followed by CID FT (summarized in Table 2). The sequencing modes CID and ETD performed similarly, whereas ETD FT provided the least number of PSMs. Considering the number of parameters that are variables for each analysis, the overall numbers are just a crude benchmark that does not provide information about each of the techniques strengths and weaknesses. Thus, we analyzed the data set of each activation method on a peptide population level, specifically at the N-acetylated, phosphorylated, and doubly, triply, and quadruply charged peptide levels.

Effect of Deconvolution

Fragmentation spectra generated by CID from precursors with charge states >2+ potentially contain multiply charged fragment ions. These multiply charged ions are often weighted lower than singly charged ions when using the Mascot search engine. Furthermore, spectra possessing multiple forms of the same fragment ion (with respect to charge state) complicate spectra and thus can cause a higher level of misassignment. These issues can be overcome by deconvolution of spectra, which increases the intensity of fragment ion peaks by summing up the intensities from their multiple charge states. Consequently, deisotoping and charge deconvolution of higher charge state peptides when using high resolution MS/MS data is required to perform a fair comparison between CID (in all forms) and ETD. For this purpose we applied the H-Score script, published recently by Savitski et al.,³⁶ to our data. The peak lists for HCD, CID FT and ETD FT were searched in Mascot both with and without deconvolution (Table 3). Not surprisingly, the number of PSMs as well as the average Mascot score increased significantly for HCD and CID FT, while the increase in PSMs for ETD FT was nominal. The limited effect of deconvolution on

Table 3. Effect of Deconvolution^a

peptide charge	HCD		CID FT		ETD FT	
	raw data	deconv.	raw data	deconv.	raw data	deconv.
2+	10037 (51)	10869 (56)	7768 (50)	8781 (61)	4320 (45)	4461 (44)
3+	4865 (38)	6698 (58)	3375 (35)	5488 (56)	3853 (56)	4055 (68)
4+	943 (30)	2470 (52)	365 (29)	2068 (49)	1676 (45)	1924 (89)

^a Deconvolution of peak list files provides for an increase in number of PSMs and average Mascot score (in brackets).

ETD FT data can partly be explained by the charge reduction of the precursor inherent to ETD, an initial step of the fragmentation process. Note that the presence of c−1 and z+1 ions due to hydrogen transfer potentially complicates the deconvolution of ETD FT spectra. All subsequent data analyses were carried out using solely the deconvoluted data.

Mascot Score Distribution

We plotted the Mascot score distribution for each peptide fragmentation mode in the five classified types of peptides (Figure 1). To be consistent we based the cutoff point for each population to correspond to an FDR of <1%, and thus the score cutoff differs between each fragmentation mode. Using this FDR, the score cutoff was lowest for HCD and highest for ETD and ETD FT. Since the mass accuracy at the MS level was similar for all modes of analysis, differences are caused by the activation technique and the type of analyzer used for the readout of fragmentation patterns. Supplemental activation after the electron transfer step improves backbone cleavage but also induces hydrogen-atom transfer from c- to z-ions.^{14,20} This mass shift of 1 Da increases the number of fragment ions that cannot be assigned by the Mascot search engine and thus leads to the higher score cutoff for the ETD modes,⁴⁰ although other search engines can accommodate the effect.⁴¹ The lower cutoff for HCD leads to a significantly higher number of spectra (and therefore peptides) being accepted that have a score between 20 and 30 compared to the other peptide activation techniques. Overall our data indicates that there is a trade-off between spectral quality and speed when using the Orbitrap. For CID, the high resolution and mass accuracy of the Orbitrap significantly increase the number of PSMs and average Mascot ion scores compared to conventional ion trap CID. The difference increases with higher charge states, which illustrates the benefit of deconvolution (Figure 1A–C). It should be noted that the superior mass accuracy and resolution of the Orbitrap will not directly increase Mascot scores but does help the peptide identification process by eliminating more false

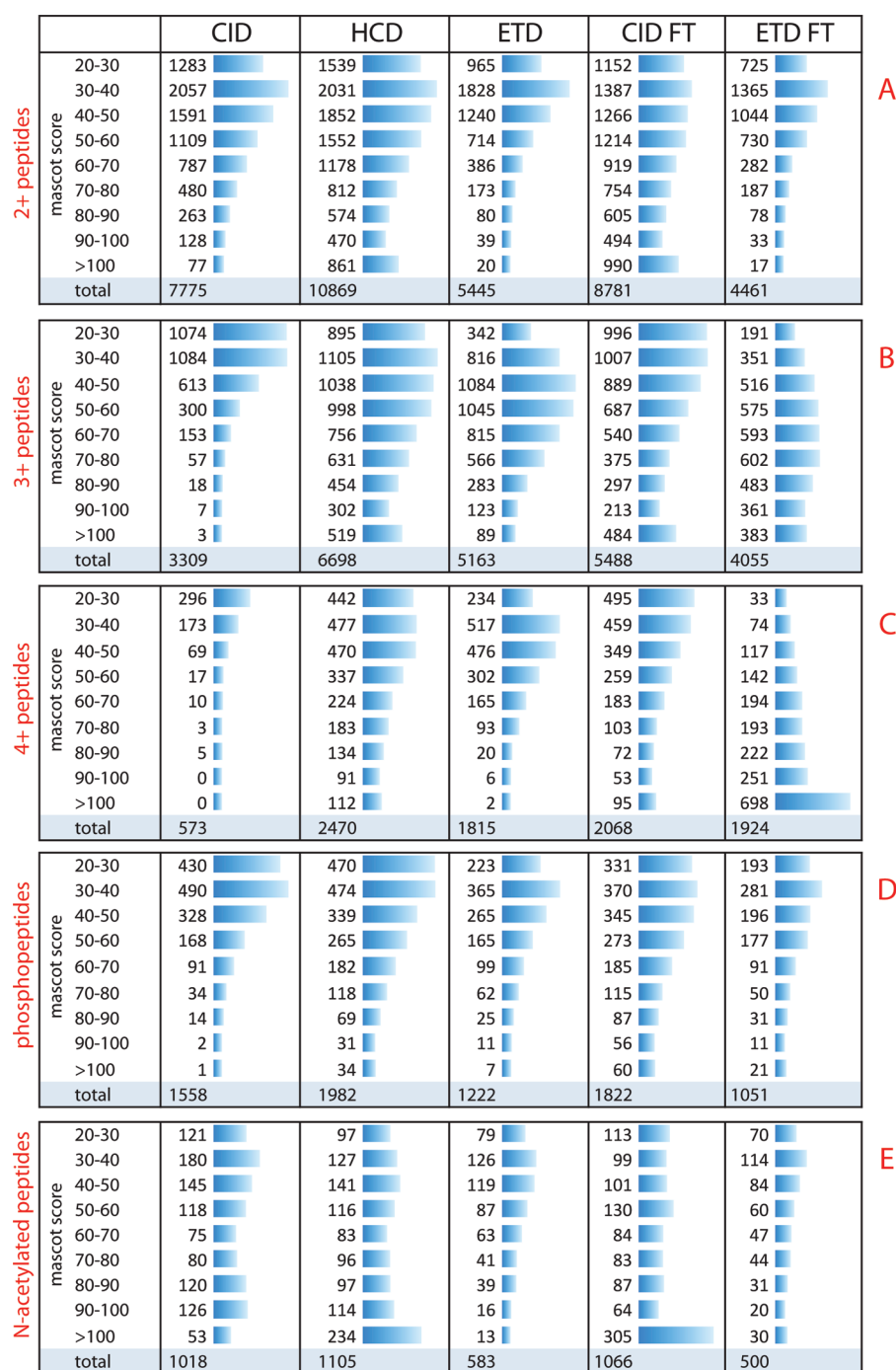


Figure 1. Histograms illustrating the Mascot ion score distribution of the doubly (A), triply (B), quadruply (C), phosphorylated (D), and N-acetylated (E) peptides that were identified from the analyses of SCX-fractionated tryptic peptides. Samples were analyzed consecutively for five times employing either CID, HCD, ETD, CID FT, or ETD FT. Data bars are normalized to the highest value within each population.

positives, i.e., a lower Mascot score can be reached with the same FDR value using higher quality tandem mass spectra.

Regular tryptic peptides contain two basic groups that are located at the N-terminus and at the C-terminal lysine or arginine, and such peptides are often doubly charged in the gas phase. Clearly for these peptides the collisional dissociation modes HCD and CID FT provide almost equally the highest number of PSMs also in the higher Mascot ion score ranges (Figure 1A). However, this result is partially helped by more peptides with lower scores being disproportionately added to the

data set at a taken threshold of 1% FDR when compared to other activation modes. The slightly lower number of PSMs for ETD FT compared to ETD can be attributed to the slower scan cycle time.

Previous studies have shown that ETD is more suitable than CID for the identification of peptides that carry more than two charges.^{14,15} Not surprisingly, for 3+ peptides the majority of the PSMs identified by ETD are in the Mascot score range of 40–60, whereas the CID and CID FT modes provide the highest number of PSMs between Mascot scores from 20 to 40 (Figure 1B). For

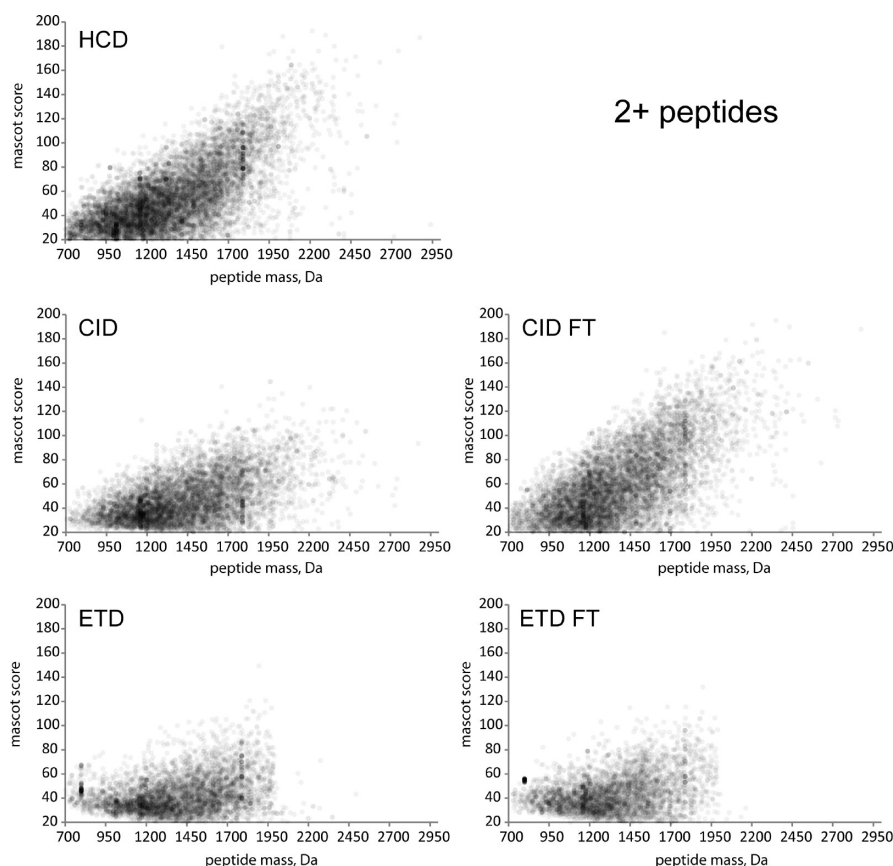


Figure 2. Density scatter plots display the influence of peptide mass on Mascot ion scores for doubly charged peptides identified from the analysis of tryptic peptides after SCX fractionation. Darker color indicates more data points.

both CID and ETD higher Mascot scores are obtained when the Orbitrap is chosen as mass analyzer. In particular, ETD FT shows a Mascot score distribution that is shifted toward higher ion scores, which is also reflected in the highest average Mascot score among all fragmentation modes. HCD provides by far the highest number of PSMs for triply charged peptides. However, the average Mascot score and Mascot score distribution is similar to ETD and CID FT. For quadruply charged peptides the Mascot score distributions for all fragmentation modes except ETD FT resemble the 3+ peptide distributions but are shifted toward lower Mascot score ranges (Figure 1C). Here, ETD FT clearly outperforms all other fragmentation modes in terms of Mascot score, providing more than one-third of all PSMs above Mascot ion scores of 100. Taking into account that the scan cycle time of ETD FT is significantly higher compared to HCD, our data suggest that ETD in combination with Orbitrap fragment ion detection provides spectra with the highest quality compared to all other fragmentation modes.

Globally, the differences in performance of the five fragmentation modes observed for the doubly charged peptides (Figure 1A) are similar in the case of phosphopeptides (Figure 1D) and N-acetylated peptides (Figure 1E). Activation with HCD provides the most PSMs followed by CID FT, CID, ETD, and ETD FT being last. The Mascot score distribution of N-acetylated peptides differs from the other peptide populations. Close inspection revealed that the high scoring PSMs observed in the data in Figure 1E originated largely from a few N-acetylated peptides that had been sequenced many times. The performance

of the ETD modes in terms of number of PSMs as well as Mascot scores is poor compared to HCD and the CID modes when analyzing N-acetylated peptides (Figure 1E, Table 2). This finding is in line with our expectations since N-acetylated peptides are less basic due to the blocked amine group at the N-terminus, which prevents protonation at this position. In summary, HCD and CID FT perform equally well for both N-acetylated and phosphopeptides in terms of number of identifications when there is a single basic amino acid present. This is in line with a recent study published by Mann and co-workers.³³

Influence of Peptide Mass on Mascot Scores

Next, we investigated the influence of peptide mass on Mascot scores for doubly, triply, and quadruply charged peptides. The general trend for doubly charged peptides is that the average Mascot score increases with peptide mass (Figure 2), which is particularly amplified for CID, CID FT, and HCD. The increase in score with mass can be explained simply by the increase in probable fragment ions with mass. For ETD and ETD FT the Mascot scores also increase with higher peptide mass but scores are, in general, significantly lower compared to the other fragmentation modes. The ETD modes provide few doubly charged PSMs with masses above 2000 Da. This cutoff seems artificial and may be attributed to supplemental activation being unable to operate on charge reduced species with m/z above 2000. In the case of triply charged peptides the influence of peptide mass on Mascot scores decreases for ion trap CID

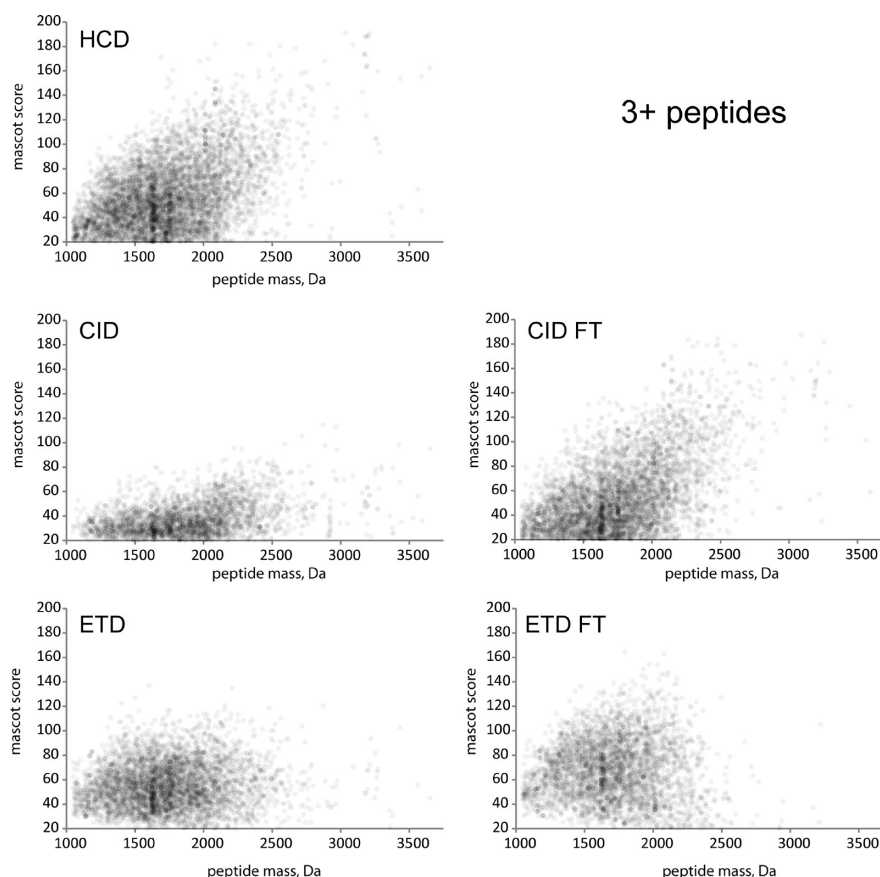


Figure 3. Density scatter plots display the influence of peptide mass on Mascot ion scores for triply charged peptides identified from the analysis of tryptic peptides after SCX fractionation. Darker color indicates more data points. Mascot ion scores increase significantly with peptide length for CID FT and HCD. The influence of peptide mass on Mascot scores is negligibly low for CID, ETD, and ETD FT.

(Figure 3). Comparing the result to CID FT indicates that deconvolution of multiply charged fragment ions is required for obtaining higher Mascot ion scores. In contrast the outcome of the fragmentation by ETD seems to be less dependent on precursor mass. Here, high and low scoring PSMs are observed over the whole mass range. Again, being able to deconvolute the ETD FT data leads to the generation of higher ion scores. However, the positive effect of deconvolution in the case of triply charged peptides analyzed by ETD FT is smaller compared to CID FT. The limited effect of deconvolution of spectra from triply charged peptides being fragmented by ETD FT can be explained by the fact that such spectra consist mostly of singly charged fragments. In general, the same holds for quadruply charged peptides (Supplemental Figure S4). The Mascot ion scores seem to be less influenced by peptide mass. For 4+ peptides the effect of deconvolution also boosts the ETD FT Mascot scores since there is now high probability of generating doubly and triply charged fragments.

Overlap in Peptide Identifications between the Fragmentation Modes

We investigated the overlap in identifications for each peptide population to examine whether fragmentation modes were either more alike or more complementary. We calculated the overlap in peptide identifications between CID, HCD, and ETD and also between CID FT, HCD, and ETD FT. We further investigated which fragmentation mode provides the highest Mascot score

from the overlapping unique peptides that were identified by all three fragmentation modes. Not surprisingly, for the doubly charged peptide population HCD provides the highest number of unique peptides (22%). Only 5% and 11% of the doubly charged peptides are exclusively identified by ETD and CID, respectively (Figure 4A). Between all three techniques 2,812 unique peptides were successfully sequenced. Within the overlap, HCD provides for 72% of these overlapping peptides the highest Mascot score followed by CID (17%) and ETD (11%). A different distribution is observed when comparing HCD, CID FT and ETD FT (Figure 4B). Here, CID FT provides for 55% of the overlapping peptides the highest Mascot score. CID FT spectra exhibit b- and y-ions over the whole mass range in contrast to HCD spectra that are dominated by y-ions. The addition of b-ions lead to higher Mascot scores, which might explain the prevalence of CID FT over HCD.

For triply charged peptides the number of unique IDs is higher for HCD compared to ETD (Figure 4C). The overlap between CID and HCD is high, whereas HCD and ETD provide more complementary unique peptide. The distribution of the highest scoring peptides within the overlap suggests that ETD can be used complementarily to HCD for peptides with charge states higher than 2. The comparison between HCD, CID FT, and ETD FT for triply charged peptides further indicates that ETD FT spectra can be considered to be more data-rich compared to HCD and CID FT as the highest Mascot score of 55% of all overlapping peptides was provided by ETD

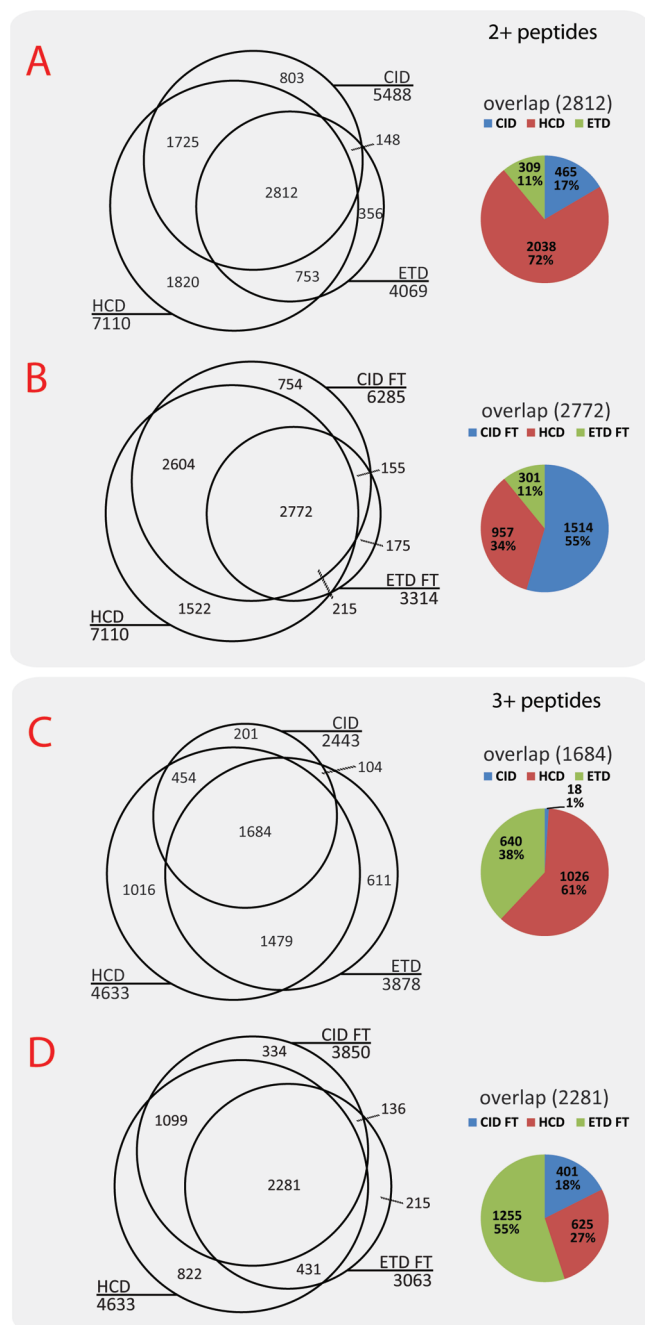


Figure 4. Overlap of the doubly (A, B) and triply (C, D) charged peptides that were identified from the SCX-fractionated tryptic HeLa digest. Venn diagrams illustrate the overlap of the unique peptides identified between CID, HCD, and ETD (A, C) and between CID FT, HCD, and ETD FT (B, D). Pie charts show the number of unique peptides with the highest Mascot score per fragmentation mode within the peptides that were identified by all three fragmentation modes.

FT (Figure 4D). Comparing ETD FT with CID FT and HCD for quadruply charged peptides shows that 82% of all peptides exhibit higher Mascot scores when sequenced by ETD FT, which clearly demonstrates the superior ability of ETD for the analysis of multiply charged peptides (Supplemental Figure S5B).

In the case of N-acetylated and singly phosphorylated peptides the distribution of the highest Mascot scores from the

overlapping unique peptides resembles the results of the regular tryptic 2+ peptides to a great extent. HCD provides the majority of the highest scoring peptides in comparison with ion trap CID and ETD (Supplemental Figures S6A, S7A) and on the other hand CID FT dominates the distribution when the FT based fragmentation modes are compared (Supplemental Figures S6B, S7B). Note, however, that a higher Mascot score by itself does not necessarily translate into improved phosphosite localization.^{19,42,43}

Analysis of a Complex Peptide Mixture

We then investigated the performance of each fragmentation mode for the analysis of non-fractionated samples. We analyzed whole human cell lysate digests directly by RP-LC-MS/MS using a 5 h LC analysis and a range of Top10 methods. Data for all acquisition modes was acquired in triplicate to investigate the repeatability of the results. The general trends for the cell lysate digests are in line with the outcome of the analyses of the SCX fractionated separate peptide pools, discussed above. In brief, HCD outperforms all other fragmentation modes followed by CID FT. The activation strategies ETD FT, ETD and CID perform approximately on the same level (Table 4, separate results from triplicate runs can be found in Supplementary Table 1). As expected the number of MS/MS spectra acquired differs largely between the fragmentation modes because of the differences in duty cycle. Interestingly, the number of PSMs does not correlate with the number of acquired MS/MS spectra. For example, the number of PSMs identified by CID and HCD differs largely, even though approximately the same number of MS/MS scans was acquired in both modes. Consequently, the success rate, defined as the number of PSMs divided by the number of MS/MS scans acquired, varies among the fragmentation modes. The highest success rate for an individual technique was obtained by HCD (49%). Not surprisingly, the ion trap detection modes clearly exhibit a lower success rate compared to the equivalent FT detection modes, which is caused both by the larger number of MS/MS spectra acquired (faster scan cycle time) and the poorer spectral quality (low resolution) of the ion trap.

Furthermore, we performed additional experiments where the amount of material analyzed was reduced to test if the apparent superior sensitivity of the linear ion trap can overcome the advantages of the high mass accuracy and resolution of the Orbitrap.²⁹ We performed equivalent analyses but now using 100 ng and 10 ng of human cell lysate. For this particular analysis, we restricted the types of analyses to HCD, CID, or ETD. The number of MS/MS spectra acquired for each activation mode is almost identical (Table 3) when analyzing these lower amounts of material, indicating that the CID mode does not benefit from the higher duty cycle of the LTQ. Strikingly, HCD results in more than twice as many PSMs as CID and three times more than ETD. This trend remains the same when analyzing 10 ng of digested human cell lysate, indicating that the improved HCD cell performs on the same level as the linear ion trap in terms of sensitivity.

We repeated the 100 ng experiment but using a shorter LC gradient (total analysis time 60 min) and Top10 methods (Table 5). Additionally, we performed a CID Top20 method. As expected, the number of MS/MS spectra acquired directly reflects the scan cycle duration of each fragmentation mode. In the CID analyses 9,021 (Top10) and 9,408 (Top20), respectively, spectra were acquired. Switching from Top10 to

Table 4. Triplicate Analysis of a Complex Peptide Mixture Derived from a Tryptic HeLa Cell Digest^a

sample load	fragmentation mode	number of PSMs	average mascot score	protein IDs	MSMS scans	success rate
1 μ g	CID	10464 \pm 420	41	1971 \pm 87	37950 \pm 567	28%
	HCD	18368 \pm 71	50	2562 \pm 31	37517 \pm 318	49%
	ETD	11007 \pm 520	41	1850 \pm 78	30182 \pm 396	36%
	CID FT	14288 \pm 352	52	2213 \pm 30	33180 \pm 549	43%
	ETD FT	11120 \pm 175	52	1878 \pm 37	25709 \pm 180	43%
	modified DDDT	18402 \pm 570	56	2586 \pm 112	33314 \pm 479	55%
	HCD	11521 \pm 275	56	2304 \pm 96	19328 \pm 340	60%
	ETD	5435 \pm 264	43	1442 \pm 77	10729 \pm 209	51%
	ETD FT	1447 \pm 46	68	717 \pm 17	3241 \pm 30	45%
	FT based DDDT	18263 \pm 323	54	2587 \pm 36	34178 \pm 285	53%
100 ng	HCD	11382 \pm 100	56	2318 \pm 22	19229 \pm 414	59%
	ETD FT	6880 \pm 258	51	1576 \pm 59	14925 \pm 142	48%
	CID	5052	42	1071	25628	20%
10 ng	HCD	12064	48	1653	24952	48%
	ETD	3738	41	740	23006	16%
	CID	1191	45	420	7372	16%
10 ng	HCD	2824	45	605	7823	36%
	ETD	859	44	315	8007	11%

^a Different amounts were analyzed over a 5 h LC gradient employing CID, CID FT, HCD, ETD, or ETD FT methods. Additionally the same sample was analyzed using the FT based and a modified decision tree method. The success rate was calculated by dividing the number of peptide identifications by the number of MS/MS scans.

Table 5. Triplicate Analysis of a Complex Peptide Mixture Using 60 min LC Gradients and Different Fragmentation Modes^a

fragmentation mode	number of PSMs	average mascot score	protein IDs	MSMS scans	success rate	max. number of MSMS events	average MSMS/sec.
CID Top10	3568 \pm 34	42	754 \pm 23	9129 \pm 180	39%	85%	4.7
CID Top20	3604 \pm 36	44	758 \pm 16	9617 \pm 191	37%	38%	5.0
HCD	5314 \pm 170	54	863 \pm 5	7615 \pm 198	70%	97%	4.0
ETD	2359 \pm 46	46	470 \pm 13	4571 \pm 115	52%	99%	2.3
CID FT	3445 \pm 52	57	618 \pm 23	5461 \pm 113	63%	99%	2.8
ETD FT	2020 \pm 26	54	410 \pm 6	3546 \pm 58	57%	99%	1.8

^a A 100 ng sample of a tryptic Hela digest was analyzed consecutively by Top10 methods employing CID, CID FT, HCD, ETD, and ETD FT. Additionally a Top20 method was set up and used for CID analysis.

Top20 had a minimal effect. Due to the slower cycle time there were fewer spectra acquired in the HCD (6,462), ETD (4,096), CID FT (4,957), and ETD FT (3,549) analyses. The average number of MS/MS scans per second was highest for CID (4.7 for Top10 and 5.0 for Top20) followed by HCD (4.0), CID FT (2.8), ETD (2.3), and ETD FT (1.8). The short LC gradient time leads to a large number of peptides coeluting at any time, and so under-sampling would be guaranteed and, in principle, there would be constant maxima of MS/MS events per cycle. Therefore, we calculated the number of MS/MS scans during each cycle over the main elution window (between RT 23.5 and 52 min of the LC gradient). All fragmentation modes except for CID were triggering the maximum number of MS/MS scans during the analysis (Table 5). In the case of CID the instrument was triggering in 85% (Top10) and 38% (Top20), respectively, of the time the maximum number of MS/MS scans per MS scan, which demonstrates the higher speed compared to the other fragmentation modes. The complexity of the sample is of such significance that it was surprising that the Top20 method was not completely maxed out. Possible reasons are poor choice of

triggering thresholds, imperfect peak picking, and insufficient dynamic range of the instrument. In an ion trap the total charge is split between all ions trapped, peptides and chemical noise. The 1 million "charges" limitation (caused by the C-trap⁴⁴) combined with the charge being distributed will lead to a compression of the dynamic range. Low abundant components will have too few charges in order to have an acceptable signal for detection. Nevertheless, the success rates of all fragmentation modes are higher for the 60 min analyses when compared to their 5 h analogues, a fact that can be explained only by the high abundant "proteotypic" precursor ions being selected for fragmentation due to the limitations in scan cycle speed. Interestingly, in terms of number of PSMs there is little difference between Top10 and Top20 CID. The Top20 method results in approximately 500 additional MS/MS spectra; however, the number of PSMs and proteins identified is on the same level. HCD still outperforms all other fragmentation modes in terms of PSMs, but in the case of CID and ETD the faster scan cycle time make the ion trap modes preferable.

Performance of a Data-Dependent Decision Tree Employing HCD, ETD, and ETD FT

Our results show that HCD performs very well for doubly charged peptides. ETD and ETD FT provided the best results in terms of Mascot score for peptides with charge states higher than two. We next investigated if it is possible to benefit from the complementary performance of the two techniques in a data-dependent fashion. Earlier, Swaney et al. showed that a data-dependent decision tree (ddDT) algorithm utilizing CID and ETD improves the sequencing success rate and generates more identifications than CID or ETD alone.²² For our experiment we initially had to choose a compromise for the instrument settings. So far, the instrument control software does not allow the programming of a ddDT logic that uses HCD with Orbitrap readout and ETD with ion trap readout because it is not possible to switch the mass analyzer used for MS/MS readout. Furthermore, we had optimized the AGC settings for each fragmentation mode for best results. Again the control software allows only one AGC value for the activation mode (regardless of the type of activation) so we chose target settings that are a compromise for HCD and ETD FT (Table 1). The FT based ddDT performs HCD for all doubly charged precursors and ETD for higher charged precursors. By addressing the most suitable fragmentation technique for each peptide we hoped to increase the number of peptide IDs, the average Mascot score and the overall success rate. We analyzed the same amount of the human cell digest (1 μ g) using the Top10 FT based decision tree HCD/ETD FT method on a 5 h gradient. In total, 34,178 MS/MS spectra were acquired where HCD contributed with 19,229 and ETD FT with 14,925 spectra. The success rates for HCD and ETD FT within the FT based ddDT are 59% and 48%, respectively. As expected, the FT based ddDT method provides about the same number of PSMs as HCD alone (Table 4). However, the average Mascot score significantly increases. Next, we modified the instrument software to allow switching between LTQ and Orbitrap analyzer and to apply separate AGC target values for the ddDT. This enabled us to use HCD, ETD and ETD FT in one single run and address every precursor by the most suitable fragmentation mode. Not surprisingly, the modified ddDT performs on the same level as HCD in terms of identified PSMs and proteins. The majority of the PSMs is provided by HCD (11,521) followed by ETD (5,435) and ETD FT (1,447). The overall success rate of 55% illustrates that more than every second MS/MS spectrum led to statistically significant peptide identification. Compared to the regular FT based ddDT, the modified one performs equally but provides slightly higher Mascot scores. Although the ddDT logic directs every precursor to either HCD, ETD, or ETD FT fragmentation, there are several peptides that were identified by multiple fragmentation modes (Figure 5). This can be explained by the fact that some peptide ions can be present in different charge states. Altogether this illustrates the feasibility of a data-dependent decision tree logic combining the advantages of different fragmentation techniques (HCD, ETD) and mass analyzers (LTQ, Orbitrap) for enhanced peptide identification.

CONCLUSION AND OUTLOOK

Our experiments were aimed to evaluate all possible combinations of fragmentation and detection modes on the current version of an Orbitrap Velos instrument. In all analyses the success rate for HCD was significantly higher than for all other modes. HCD performs best for doubly charged peptides, singly

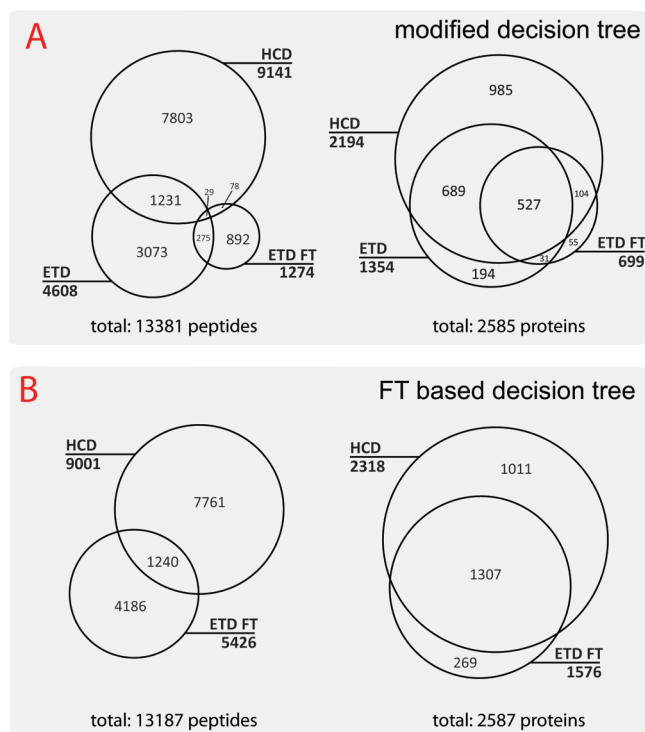


Figure 5. Venn diagrams illustrating the contribution of the different fragmentation in terms of unique peptides and proteins for the FT based ddDT (A) and modified ddDT (B).

phosphorylated peptides, and N-acetylated peptides. ETD FT outperforms the other techniques for peptides with charges states >2 in terms of Mascot scores. We found that the spectral quality of Orbitrap detection data is superior to ion trap data, especially when considering charge deconvolution. However, the main discriminating factor for obtaining the highest number of PSMs is scan cycle speed, as indicated by the larger number of identified PSMs from HCD fragmentation when compared to ETD FT. We showed that, despite the high sensitivity of the dual pressure linear ion trap, HCD still generates better results than CID even for very low amounts of peptides. We expect that ETD FT will benefit dramatically from further improvements in speed and product ion transmission from the ion trap to the Orbitrap. We further expect that a dynamic AGC parameter dependent on precursor charge and m/z value could improve the success rate for multiply charged peptides. The number of possibly observable fragment ions increases with increasing peptide length and charge state. Consequently, the product ion signal-to-noise ratio gets worse. Higher AGC values for peptides with higher charges states and m/z could help compensate for this. Assigning the peptides to the most suitable fragmentation mode is a key challenge for obtaining the highest number of PSMs. We showed that a modified data-dependent decision tree method employing HCD, ETD, and ETD FT performs similar to HCD alone for the analysis of a complex peptide mixture but provides a higher average Mascot score.

ASSOCIATED CONTENT

Supporting Information

Schematic representation of the probabilistic modified decision tree algorithm; analytical charts of Mascot data generated

from one of the LCMS analyses; example MS base peak chromatograms of five consecutive analyses using the different fragmentation modes illustrating the high repeatability of the LC separation; density scatter plots displaying the influence of peptide mass on Mascot scores for quadruply charged peptides; overlap of the quadruply charged, N-acetylated, and phosphorylated peptides that were identified from the SCX-fractionated tryptic HeLa digest; table of the number of PSMs identified for each activation technique with respect to individual LCMS analyses and for all analyses. All data are available as a scaffold file on tranche at <https://proteomecommons.org> using the following hash: L0u/QC4fuLOfEI43/5+Aea2ko37cIzjOU4lfSaSrZxID9DmXcUvo1TFD7HYus8 V3YRKX9/Hg0lIpXySt2-q5SJ2BOEbMAAAAAAABdw==. This material is available free of charge via the Internet at <http://pubs.acs.org>.

AUTHOR INFORMATION

Corresponding Author

*E-mail: s.mohammed@uu.nl or a.j.r.heck@uu.nl.

ACKNOWLEDGMENT

This research was performed within the framework of CTMM, the Center for Translational Molecular Medicine (www.ctmm.nl), project CIRCULATING CELLS (grant 01C-102), and supported by The Netherlands Heart Foundation. Additionally, The Netherlands Proteomics Centre, a program embedded in The Netherlands Genomics Initiative, is kindly acknowledged for financial support.

ABBREVIATIONS

CID, collision induced dissociation; TOF, time-of-flight; QqQ, triple quadrupole; QqTOF, quadrupole time-of-flight; Q-TRAP, quadrupole linear ion trap; ECD, electron capture dissociation; ETD, electron transfer dissociation; FT-ICR, Fourier-transform ion cyclotron resonance; MS/MS, tandem mass spectrometry; HCD, higher-energy collisional dissociation; SCX, strong cation exchange; FT, Orbitrap readout; PSM, peptide spectrum match; AGC, automatic gain control; FDR, false discovery rate

REFERENCES

- (1) Washburn, M. P.; Wolters, D.; Yates, J. R., 3rd Large-scale analysis of the yeast proteome by multidimensional protein identification technology. *Nat. Biotechnol.* **2001**, *19* (3), 242–7.
- (2) Hunt, D. F.; Yates, J. R., 3rd; Shabanowitz, J.; Winston, S.; Hauer, C. R. Protein sequencing by tandem mass spectrometry. *Proc. Natl. Acad. Sci. U.S.A.* **1986**, *83* (17), 6233–7.
- (3) Vachet, R. W.; Ray, K. L.; Glish, G. L. Origin of product ions in the MS/MS spectra of peptides in a quadrupole ion trap. *J. Am. Soc. Mass Spectrom.* **1998**, *9* (4), 341–4.
- (4) Lau, K. W.; Hart, S. R.; Lynch, J. A.; Wong, S. C.; Hubbard, S. J.; Gaskell, S. J. Observations on the detection of b- and y-type ions in the collisionally activated decomposition spectra of protonated peptides. *Rapid Commun. Mass Spectrom.* **2009**, *23* (10), 1508–14.
- (5) Syka, J. E.; Coon, J. J.; Schroeder, M. J.; Shabanowitz, J.; Hunt, D. F. Peptide and protein sequence analysis by electron transfer dissociation mass spectrometry. *Proc. Natl. Acad. Sci. U.S.A.* **2004**, *101* (26), 9528–33.
- (6) Zubarev, R. A. Electron-capture dissociation tandem mass spectrometry. *Curr. Opin. Biotechnol.* **2004**, *15* (1), 12–6.
- (7) Xia, Y.; Chrisman, P. A.; Erickson, D. E.; Liu, J.; Liang, X.; Londry, F. A.; Yang, M. J.; McLuckey, S. A. Implementation of ion/ion

reactions in a quadrupole/time-of-flight tandem mass spectrometer. *Anal. Chem.* **2006**, *78* (12), 4146–54.

- (8) Pitteri, S. J.; Chrisman, P. A.; Hogan, J. M.; McLuckey, S. A. Electron transfer ion/ion reactions in a three-dimensional quadrupole ion trap: reactions of doubly and triply protonated peptides with SO₂⁺. *Anal. Chem.* **2005**, *77* (6), 1831–9.

- (9) McAlister, G. C.; Berggren, W. T.; Griep-Raming, J.; Horning, S.; Makarov, A.; Phanstiel, D.; Stafford, G.; Swaney, D. L.; Syka, J. E.; Zabrouskov, V.; Coon, J. J. A proteomics grade electron transfer dissociation-enabled hybrid linear ion trap-orbitrap mass spectrometer. *J. Proteome Res.* **2008**, *7* (8), 3127–36.

- (10) Kaplan, D. A.; Hartmer, R.; Speir, J. P.; Stoermer, C.; Gumerov, D.; Easterling, M. L.; Brekenfeld, A.; Kim, T.; Laukien, F.; Park, M. A. Electron transfer dissociation in the hexapole collision cell of a hybrid quadrupole-hexapole Fourier transform ion cyclotron resonance mass spectrometer. *Rapid Commun. Mass Spectrom.* **2008**, *22* (3), 271–8.

- (11) Satake, H.; Hasegawa, H.; Hirabayashi, A.; Hashimoto, Y.; Baba, T.; Masuda, K. Fast multiple electron capture dissociation in a linear radio frequency quadrupole ion trap. *Anal. Chem.* **2007**, *79* (22), 8755–61.

- (12) Axelsson, J.; Palmblad, M.; Hakansson, K.; Hakansson, P. Electron capture dissociation of substance P using a commercially available Fourier transform ion cyclotron resonance mass spectrometer. *Rapid Commun. Mass Spectrom.* **1999**, *13* (6), 474–7.

- (13) Altelaar, A. F.; Mohammed, S.; Brans, M. A.; Adan, R. A.; Heck, A. J. Improved identification of endogenous peptides from murine nervous tissue by multiplexed peptide extraction methods and multiplexed mass spectrometric analysis. *J. Proteome Res.* **2009**, *8* (2), 870–6.

- (14) Swaney, D. L.; McAlister, G. C.; Wirtala, M.; Schwartz, J. C.; Syka, J. E.; Coon, J. J. Supplemental activation method for high-efficiency electron-transfer dissociation of doubly protonated peptide precursors. *Anal. Chem.* **2007**, *79* (2), 477–85.

- (15) Good, D. M.; Wirtala, M.; McAlister, G. C.; Coon, J. J. Performance characteristics of electron transfer dissociation mass spectrometry. *Mol. Cell. Proteomics* **2007**, *6* (11), 1942–51.

- (16) van den Toorn, H. W. P.; Mohammed, S.; Gouw, J. W.; van Breukelen, B.; Heck, A. J. R. Targeted SCX based peptide fractionation for optimal sequencing by collision induced, and electron transfer dissociation. *J. Proteomics Bioinform.* **2008**, *1* (8), 379–88.

- (17) Mikesch, L. M.; Ueberheide, B.; Chi, A.; Coon, J. J.; Syka, J. E.; Shabanowitz, J.; Hunt, D. F. The utility of ETD mass spectrometry in proteomic analysis. *Biochim. Biophys. Acta* **2006**, *1764* (12), 1811–22.

- (18) Wiesner, J.; Premisler, T.; Sickmann, A. Application of electron transfer dissociation (ETD) for the analysis of posttranslational modifications. *Proteomics* **2008**, *8* (21), 4466–83.

- (19) Boersema, P. J.; Mohammed, S.; Heck, A. J. Phosphopeptide fragmentation and analysis by mass spectrometry. *J. Mass Spectrom.* **2009**, *44* (6), 861–78.

- (20) Molina, H.; Matthiesen, R.; Kandasamy, K.; Pandey, A. Comprehensive comparison of collision induced dissociation and electron transfer dissociation. *Anal. Chem.* **2008**, *80* (13), 4825–35.

- (21) Taouatas, N.; Altelaar, A. F.; Drugan, M. M.; Helbig, A. O.; Mohammed, S.; Heck, A. J. Strong cation exchange-based fractionation of Lys-N-generated peptides facilitates the targeted analysis of post-translational modifications. *Mol. Cell. Proteomics* **2009**, *8* (1), 190–200.

- (22) Swaney, D. L.; McAlister, G. C.; Coon, J. J. Decision tree-driven tandem mass spectrometry for shotgun proteomics. *Nat. Methods* **2008**, *5* (11), 959–64.

- (23) Makarov, A.; Denisov, E.; Kholomeev, A.; Balschun, W.; Lange, O.; Strupat, K.; Horning, S. Performance evaluation of a hybrid linear ion trap/orbitrap mass spectrometer. *Anal. Chem.* **2006**, *78* (7), 2113–20.

- (24) Olsen, J. V.; Macek, B.; Lange, O.; Makarov, A.; Horning, S.; Mann, M. Higher-energy C-trap dissociation for peptide modification analysis. *Nat. Methods* **2007**, *4* (9), 709–12.

- (25) Zhang, Y.; Ficarro, S. B.; Li, S.; Marto, J. A. Optimized Orbitrap HCD for quantitative analysis of phosphopeptides. *J. Am. Soc. Mass Spectrom.* **2009**, *20* (8), 1425–34.

- (26) Kocher, T.; Pichler, P.; Schutzbier, M.; Stingl, C.; Kaul, A.; Teucher, N.; Hasenfuss, G.; Penninger, J. M.; Mechtler, K. High precision quantitative proteomics using iTRAQ on an LTQ Orbitrap: a new mass spectrometric method combining the benefits of all. *J. Proteome Res.* **2009**, *8* (10), 4743–52.
- (27) Mischerikow, N.; van Nierop, P.; Li, K. W.; Bernstein, H. G.; Smit, A. B.; Heck, A. J.; Altelaar, A. F. Gaining efficiency by parallel quantification and identification of iTRAQ-labeled peptides using HCD and decision tree guided CID/ETD on an LTQ Orbitrap. *Analyst* **2010**, *135* (10), 2643–52.
- (28) Zhang, J.; Wang, Y.; Li, S. Deuterium isobaric amine-reactive tags for quantitative proteomics. *Anal. Chem.* **2010**, *82* (18), 7588–95.
- (29) Olsen, J. V.; Schwartz, J. C.; Griep-Raming, J.; Nielsen, M. L.; Damoc, E.; Denisov, E.; Lange, O.; Remes, P.; Taylor, D.; Splendore, M.; Wouters, E. R.; Senko, M.; Makarov, A.; Mann, M.; Horning, S. A dual pressure linear ion trap Orbitrap instrument with very high sequencing speed. *Mol. Cell. Proteomics* **2009**, *8* (12), 2759–69.
- (30) Second, T. P.; Blethrow, J. D.; Schwartz, J. C.; Merrihew, G. E.; MacCoss, M. J.; Swaney, D. L.; Russell, J. D.; Coon, J. J.; Zabrouskov, V. Dual-pressure linear ion trap mass spectrometer improving the analysis of complex protein mixtures. *Anal. Chem.* **2009**, *81* (18), 7757–65.
- (31) Sobott, F.; Watt, S. J.; Smith, J.; Edelman, M. J.; Kramer, H. B.; Kessler, B. M. Comparison of CID versus ETD based MS/MS fragmentation for the analysis of protein ubiquitination. *J. Am. Soc. Mass Spectrom.* **2009**, *20* (9), 1652–9.
- (32) Scott, N. E.; Parker, B. L.; Connolly, A. M.; Paulech, J.; Edwards, A. V.; Crossett, B.; Falconer, L.; Kolarich, D.; Djordjevic, S. P.; Hojrup, P.; Packer, N. H.; Larsen, M. R.; Cordwell, S. J. Simultaneous glycan-peptide characterization using hydrophilic interaction chromatography and parallel fragmentation by CID, HCD and ETD-MS applied to the N-linked glycoproteome of *Campylobacter jejuni*. *Mol. Cell. Proteomics* **2010**, *10*, M000031MCP201.
- (33) Nagaraj, N.; D'Souza, R. C.; Cox, J.; Olsen, J. V.; Mann, M. Feasibility of large scale phosphoproteomics with higher energy collisional dissociation fragmentation. *J. Proteome Res.* **2010**, *9*, 6786–94.
- (34) McAlister, G. C.; Phanstiel, D.; Wenger, C. D.; Lee, M. V.; Coon, J. J. Analysis of tandem mass spectra by FTMS for improved large-scale proteomics with superior protein quantification. *Anal. Chem.* **2010**, *82* (1), 316–22.
- (35) Gauci, S.; Helbig, A. O.; Slijper, M.; Krijgsveld, J.; Heck, A. J.; Mohammed, S. Lys-N and trypsin cover complementary parts of the phosphoproteome in a refined SCX-based approach. *Anal. Chem.* **2009**, *81* (11), 4493–501.
- (36) Savitski, M. M.; Mathieson, T.; Becher, I.; Bantscheff, M. H-score, a mass accuracy driven rescoring approach for improved peptide identification in modification rich samples. *J. Proteome Res.* **2010**, *9* (11), 5511–6.
- (37) Green, B. N.; Hutton, T.; Vinogradov, S. N. Analysis of complex protein and glycoprotein mixtures by electrospray ionization mass spectrometry with maximum entropy processing. *Methods Mol. Biol.* **1996**, *61*, 279–94.
- (38) van den Toorn, H. W.; Munoz, J.; Mohammed, S.; Raijmakers, R.; Heck, A. J.; van Breukelen, B. RockerBox: analysis and filtering of massive proteomics search results. *J. Proteome Res.* **2010**, *10*, 1420–4.
- (39) Kall, L.; Canterbury, J. D.; Weston, J.; Noble, W. S.; MacCoss, M. J. Semi-supervised learning for peptide identification from shotgun proteomics datasets. *Nat. Methods* **2007**, *4* (11), 923–5.
- (40) Sun, R. X.; Dong, M. Q.; Song, C. Q.; Chi, H.; Yang, B.; Xiu, L. Y.; Tao, L.; Jing, Z. Y.; Liu, C.; Wang, L. H.; Fu, Y.; He, S. M. Improved peptide identification for proteomic analysis based on comprehensive characterization of electron transfer dissociation spectra. *J. Proteome Res.* **2010**, *9*, 6354–67.
- (41) Kim, S.; Mischerikow, N.; Bandeira, N.; Navarro, J. D.; Wich, L.; Mohammed, S.; Heck, A. J.; Pevzner, P. A. The generating function of CID, ETD, and CID/ETD pairs of tandem mass spectra: applications to database search. *Mol. Cell. Proteomics* **2010**, *9* (12), 2840–52.
- (42) Mischerikow, N.; Altelaar, A. F.; Navarro, J. D.; Mohammed, S.; Heck, A. J. Comparative assessment of site assignments in CID and electron transfer dissociation spectra of phosphopeptides discloses limited relocation of phosphate groups. *Mol. Cell. Proteomics* **2010**, *9* (10), 2140–8.
- (43) Palumbo, A. M.; Smith, S. A.; Kalcic, C. L.; Dantus, M.; Stemmer, P. M.; Reid, G. E. Tandem mass spectrometry strategies for phosphoproteome analysis. *Mass Spectrom. Rev.* **2011**, Epub ahead of print; DOI: 10.1002/mas.20310.
- (44) Makarov, A.; Denisov, E.; Lange, O.; Horning, S. Dynamic range of mass accuracy in LTQ Orbitrap hybrid mass spectrometer. *J. Am. Soc. Mass Spectrom.* **2006**, *17* (7), 977–82.